Development and testing of a domestic woodstove thermoelectric generator with natural convection cooling

Rida Y. Nuwayhid, Alan Shihadeh *, Nesreen Ghaddar

Faculty of Engineering and Architecture, Department of Mechanical Engineering, American University of Beirut, P.O. Box 11-0236, Raid El Solh, Beirut, Lebanon

Abstract

A thermoelectric generator was fitted to the side of a domestic woodstove. The generator was driven using one or more thermoelectric modules designed to give significant power at a reasonable cost. The thermoelectric generator was air cooled by natural convection using a commercially available heat sink. Testing was undertaken under a controlled woodstove firing rate and temperatures, and open circuit voltages were monitored over extended periods. The maximum steady state matched load power was 4.2 W using a single module. The use of multiple modules with a single heat sink was found to reduce the total power output relative to the single module case as a result of reduced hot to cold surface temperature differences.
© 2004 Elsevier Ltd. All rights reserved.

Keywords: Woodstove; Thermoelectric generator; Natural convection

1. Introduction

With relatively cold winters, biomass or wood fired domestic stoves (called in local Arabic "Suba" or "Wujak") are commonly used for space heating and cooking in the homes of rural Lebanon. At the same time, the national utility company has failed to provide reliable electric

---

power, especially in rural areas. One option for attaining off the grid distributed power generation in the cold months may be to retrofit existing domestic stoves with low cost thermoelectric generators.

Thermoelectric power generation has the advantages of being maintenance free, silent in operation and involving no moving or complex parts. It is well suited to take advantage of low grade waste heat. With current thermoelectric efficiencies of 5–10%, the heat rejected from the thermoelectric generator (TEG) goes back to room heating. Since improvement in room heating may be an added side benefit, depending on the heat rejection method, the process can be considered "cogeneration". Recently, Min and Rowe [1] described theoretically a domestic water boiler coupled with a TEG as a "symbiotic" system and showed that the efficiency of the combined system is equal to that of the heating system alone with the added electricity as a bonus. The domestic woodstove coupled to an efficient TEG may also qualify as a symbiotic system and, with the recent drop in thermoelectric materials prices, may thus be an economically feasible proposition in favorable locations.

The application of a thermoelectric generator to a rural stove was first described by Kilander and Bass [2] in a study for extreme North Sweden where electric power lines are non-existent. Nuwayhid et al. [3] considered the prospect of applying TEG/stoves to rural Lebanon where the electric supply is unreliable and subject to frequent disruption but where the management of pine, oak and other woods can provide sustainable sources of wood for fueling domestic stoves.

In the work described below, the use of a thermoelectrically outfitted woodstove is envisaged to provide a continuous 10–100 W electric power supply in the course of its primary use as a home heater.

The aims of this work were to (a) develop a low cost, high performance TEG module and (b) to test the TEG in various configurations using a common wood burning stove and an off the shelf finned heat sink in order to determine the performance potential of this simple system.

2. Thermoelectric power generation

2.1. Thermoelectric background

The thermoelectric effect was apparently first discovered in 1822 by Seebeck, who observed an electric flow when one junction of two dissimilar metals, joined at two places, was heated while the other junction was kept at a lower temperature [4]. The output produced was initially of a small magnitude and was of no value in electric power generation. With the discovery of semiconductors, it was found that the output could be magnified significantly and renewed interest began around the middle of the 20th century [5].

Fig. 1 provides a schematic of the operation of a thermoelectric (TE) generator, where the dissimilar materials are designated p and n to reflect that one has an excess and one a deficiency of electrons, respectively. The parameter giving the output voltage for a given p–n junction for a certain temperature difference is the "Seebeck coefficient": $\alpha = dV/dT$. Seebeck coefficients of metals are in the range 0–50 μV/K, while that for semiconductors could be over 300 μV/K [6].
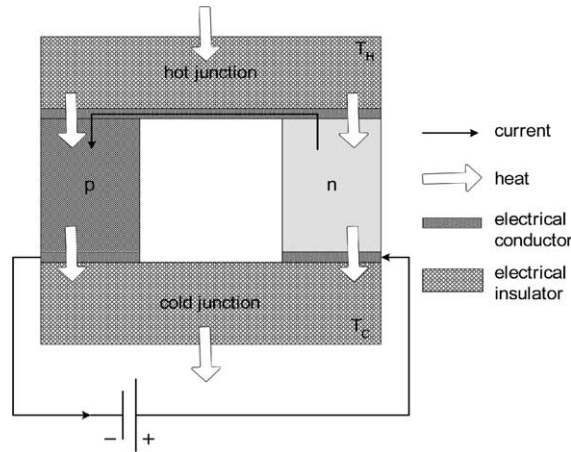
Fig. 1. Schematic of a single thermoelectric couple.

2.2. Power relations

The equations governing the heat input rate, heat output rate and the power produced per couple operating between the hot side T_H and the cold side T_C are obtained by energy balances around the hot junction and cold junction, respectively [7,8]:

$$
\begin{aligned}
Q_{in} &= 2\alpha I T_H + \frac{2kA}{L}(\Delta T) - \frac{1}{2}I^2\frac{2\rho L}{A} \\
Q_{out} &= 2\alpha I T_C + \frac{2kA}{L}(\Delta T) + \frac{1}{2}I^2\frac{2\rho L}{A}
\end{aligned}
\tag{1}
$$

An energy balance around the whole couple $P = Q_{in} - Q_{out}$ leads to

$$
P = 2\left(\alpha I \Delta T - I^2\frac{\rho L}{A}\right)
\tag{2}
$$

where ΔT is $T_H - T_C$, A is the area of the thermoelement (leg), L is its length, k is the thermal conductivity, ρ is the electrical resistivity and I is the electrical current. It has been assumed that the Seebeck coefficient, the thermal conductivity and the electrical resistivity of the n and p legs are approximately the same (thus the factor 2).

The open circuit voltage is given by

$$
V_{oc} = 2\alpha\Delta T
\tag{3}
$$

The electrical current is then given by Ohms law:

$$
I = \frac{\alpha A \Delta T}{\rho L(1 + m)}
\tag{4}
$$

where $m = R_L/R$ is the load ratio and R_L is the external load resistance.

Inserting the current into Eq. (2) gives the power output in terms of material and geometric properties for a given temperature difference:

$$p_{max} = 2 \frac{m}{(1+m)^2} \frac{\alpha^2}{\rho} \frac{A}{L} \Delta T^2 \tag{5}$$

Using the above relations and considering that a thermoelectric module contains N couples, we have, for the limiting open circuit; short circuit and maximum power cases, the following relations:

$$V_{oc} = 2\alpha N \Delta T \tag{6}$$

$$V_{mp} = \frac{V_{oc}}{2} = \alpha N \Delta T \tag{7}$$

$$I_{sc} = \frac{\alpha}{\rho} \frac{A}{L} \Delta T \tag{8}$$

$$I_{mp} = \frac{1}{2} \frac{\alpha}{\rho} \frac{A}{L} \Delta T \tag{9}$$

$$p_{max} = \frac{1}{2} \frac{\alpha^2}{\rho} \frac{NA}{L} \Delta T^2 \tag{10}$$

Power is thus a function of the temperature difference applied, the geometry of the generator (N, A and L) and the material characteristics (α and ρ). Thus, the greater α^2/ρ, the power factor, the higher the power output for a given combination of thermoelectric p and n materials will be.

3. Thermoelectric power module design

TEG modules available in the market are generally too costly for the application envisaged here. As a result, the task was to design and manufacture a TEG module at relatively low cost, which is capable of producing as much (or more) power than commercially available modules.

A comparison of several available modules together with the proposed new one was made. The relations used for the open circuit voltage, the voltage at maximum power (V_{mp}), the current at maximum power (I_{mp}) and the maximum power (P_m) are useful indicators of performance.

Of the several commercially available thermoelectric materials, doped bismuth telluride (Bi_2Te_3) exhibits the highest power factor ($37 \times 10^{-4}\,W/mK^2$) in the 20 °C to 300 °C temperature range and is, therefore, the most widely used in such applications [6]. It was, therefore, chosen for the current design. For bismuth telluride, the appropriately averaged temperature-range Seebeck coefficient, electrical resistivity and thermal conductivity are conservatively taken as 190 µV/K, $1.6 \times 10^{-5}\,\Omega m$ and 1.5 W/m K [8]. Using the relations of the previous section, the open circuit voltage, maximum power voltage, maximum power current and the maximum power are then given by

$$V_{oc} = 2 \times 190 \times 10^{-6} N\Delta T$$

$$V_{mp} \cong 190 \times 10^{-6} N\Delta T$$

$$I_{mp} \cong 0.06 \frac{A}{L}\Delta T \tag{11}$$

$$P_{m} \cong 0.114 \times 10^{-4} \frac{A}{L} N\Delta T^2$$

where N is the number of couples in the module, A is the thermoelement (single leg) area in square centimetre, L is the thermoelement length in centimetre and ΔT is the available temperature difference across the TE module.

While the above equation for maximum power indicates that as the leg length (L) decreases, power should increase, it fails for very short lengths. An improved relation due to Min and Rowe [9] includes the effect of increasing contact resistance and shows an optimum length for maximum power to be obtained. This equation can be written as

$$P_{m} \cong 0.114 \times 10^{-4} \frac{A}{(L+n)(1+2r\frac{l_c}{L})^2} N\Delta T^2 \tag{12}$$

where l_c is the thickness of the insulating layer(s) and $r(=k/k_c)$ and $n(=2\rho_c/\rho)$ are the ratios of the thermal contact and electrical resistivities, respectively. It is thus seen that reducing leg height can lead to an increase in power output (although the efficiency may be slightly reduced). In designing the new unit, it was, therefore, decided to use a small leg length together with a sufficient number of couples and leg area to maximize power output.

Table 1 lists the essential geometric and performance features of several representative commercially available power modules as well as the AUB design (TEP-AUB) and the resultant as built variant (TEP-12656), which was manufactured at Thermanomic Electronics Co. (Xiamen, China). Because of manufacturing constraints, the as built unit TEP-12656 differs from the TEP-AUB in the number of couples and leg length. The new module has an overall size of 56 mm × 56 mm, falling between the usual Peltier module sizes (40 mm × 40 mm) and the larger commercial power modules (75 mm × 75 mm). The predicted electric performance at maximum power (matched load) of the TEP-12656 is similar to the initial design TEP-AUB and both significantly out perform the

Table 1
Geometric characteristics and theoretical performance of modules

Module model/ manufacturer	Leg length (L), cm	Leg area (A), cm²	Couples (N)	$V_{mp}/\Delta T$, V/K	$I_{mp}/\Delta T$, A/K	Power density $P_{m}/\Delta T^2/A_s \times 10^6$ W/K²/cm²	Cost $/W for $\Delta T = 150$ K
HZ-20/Hi-Z, Inc (USA)	0.50	0.30	71	0.0135	0.036	8.71	15–20
TEP1-12708 Thermanomic Electronics (China)	0.125	0.0196	127	0.024	0.01	15.0	1–2
TEP-AUB	0.14	0.0625	127	0.0241	0.027	20.7	2–5
TEP-12656	0.15	0.0625	126	0.0239	0.025	19.1	2–5

Last two columns indicate theoretical power per surface area and cost of each TE module. Higher cost figures reflect current individual unit market price, while lower figure represents manufacturer's reported minimum price for high number production.

commercially available units, as indicated by their higher surface area normalized $P_m/\Delta T^2$ values shown in Table 1.

4. Heat rejection and predicted TEG performance

For a given TEG design and hot surface temperature, the problem becomes one of maximizing heat rejection from the TEG cold side to the relatively cool surroundings. In particular, the lower the heat transfer resistance from the TEG to the surrounding air, the lower the cold side temperature will be, and the greater the TEG electrical output will be. While many options are possible, the simplest readily available heat rejection device that could be readily utilized in a household environment is the natural convection finned heat sink. To this end, a high performance heat fin type heat sink was sought from commercial sources in a configuration that would accommodate three TEG modules per heat sink. A high performance extruded aluminum heat sink manufactured by Wakefield, Inc. (USA) was selected based on its low natural convection thermal resistance R_{HS}, of 0.43 °C/W. It has an 18 cm long by 12.5 cm wide base, and the fin structure protrudes 136 mm from the mating surface. These dimensions were deemed to be within practical limits for a household stove TEG retrofit. Other natural convection heat sink types are available such as the bonded or folded fin type, which offer thinner and, therefore, higher performance fins, but extruded aluminum heat sinks offer a higher performance/price ratio.

The nominal thermal resistance of 0.43 °C/W of the heat sink, combined with the TEG thermal resistance, R_{TEG} of

$$R_{TEG} = \frac{\Delta x}{kA} = \frac{0.37\,\text{cm}}{0.024\,\frac{\text{W}}{\text{cm K}}\,(31\,\text{cm}^2)} = 0.49\,\frac{°\text{C}}{\text{W}} \tag{13}$$

yields, for a nominal operating condition of 250 °C hot side and 20 °C ambient, a heat transfer rate of $\dot{Q} = \frac{\Delta T}{R_{TEG}+R_{Hs}} = 250\,\text{W}$ and a cold side TEG temperature of 128 °C, where Δx, k and A refer to the TE module thickness, thermal conductivity and cross-sectional surface area, respectively. The best possible temperature drop across the TE module due to natural convection alone will thus be approximately 120 °C. In practice, the temperature drop will be less due to contact resistances between the various mating surfaces, as well as the expected reduction in cooling efficiency of the heat sink, which would result from the fact that rather than being distributed evenly over the entire heat sink base (18 cm × 12.5 cm), the heat transferred through the sink will be concentrated in a 56 mm × 56 mm region corresponding to the TE module dimensions. A 120 °C temperature difference is expected to yield a maximum power output of 9.2 W for the TEP-12656 module.

In the case of N identical modules mounted side by side under the same heat sink, it can be shown that $\dot{Q} = \frac{\Delta T_{H\infty}}{\frac{R_{TEG}}{N}+R_{HS}}$ where $\Delta T_{H\infty}$ refers to the temperature difference between the hot side of the TE module and the ambient air. Using the previously given relations, the maximum (i.e. matched load) power output for the AUB-12656 modules connected in series is thus given by $P_{max} = 2.28 \times 10^{-3} \frac{N^2 R_{TEG}}{(N+1)^2(R_{TEG}+R_C+NR_{HS})^2}\Delta T_{H\infty}^2$, where R_C refers to net contact resistance for all the heat transfer interfaces. It follows that the open circuit voltage achieved with N modules
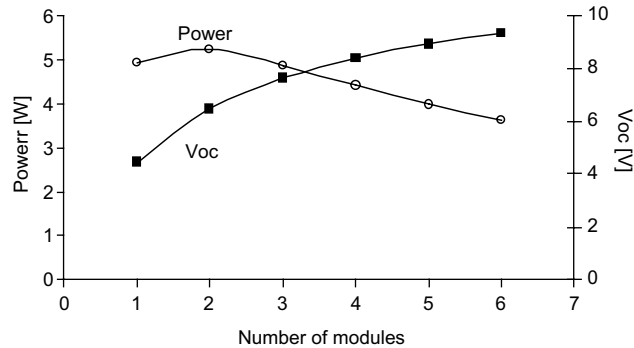
Fig. 2. Predicted net maximum power and open circuit voltage, V_{oc}, as a function of number of modules mounted under a single heat sink.

relative to that achieved with one module for a given heat sink and a given hot surface to ambient temperature is approximately given by

$$V_N = V_1 \frac{N(R_{TEG} + R_C + R_{HS})}{R_{TEG} + R_C + NR_{HS}} \tag{14}$$

The theoretical power output and open circuit voltage, assuming zero interfacial contact resistances, are plotted in Fig. 2 for a hot surface to ambient temperature difference of 250 °C, where it can be seen that the maximum power is reached when two modules are mounted per heat sink. As more modules are used, the heat sink must reject more heat to the ambient surroundings, causing the cold side temperature to increase, thereby decreasing the temperature differential across the TEG modules. Thus, the reduction in temperature difference more than offsets the benefit of increasing the number of modules beyond two. On the other hand, while three modules are not preferable to one in terms of power output, the higher operating voltage of the three module system may be more practical for an application with limited voltage conditioning capabilities.

5. Experimental

5.1. Woodstove

Most woodstoves in use in rural Lebanon are manufactured locally and are typically of the heating–cooking type, similar to that shown in Fig. 3. The stoves have ample top surface area for pan cooking or water boiling as well as a baking compartment adjacent to the firebox. They typically come in two variants; one welded from light steel, the other thick walled cast iron. Local market prices are approximately $60 and $100 for the two types, respectively. For this study, the cast iron stove was used, primarily for its considerably greater thermal inertia, which would help dampen temperature fluctuations arising as a result of the combustion process. The weight and relevant dimensions are given in Table 2.

To standardize the experiments, soft pine wood blocks of approximate dimension 2 cm × 6 cm × 15 cm were used in the stove and fed at a nominal rate of 2.5 kg/h in 15 min

Fig. 3. Woodstove used in this study. Dimensions are given in Table 2.

Table 2
Stove properties

Construction material	Cast iron
Weight (kg)	40 (approx.)
Height (cm)	29
Width (cm)	44.5
Depth (cm)	52
Wall thickness (cm)	0.5 (sides) 1.5 (top)
Flue diameter (cm)	12

intervals. At an ambient temperature of 19 °C, the maximum feeding rate was found to be 3.15 kg/h and the minimum required to sustain continuous combustion was 2 kg/h. For each experiment, the stove was initially fired at the maximum feeding rate to achieve rapidly the normal operating temperatures. Once the stove temperatures approached the desired values, wood was fed at the nominal rate and steady state conditions were awaited. Steady state was considered achieved when the temperatures at two non-sensitive (i.e. thermally damped) locations no longer changed. These locations were chosen on the side of the stove where there is no direct contact with the flame.

5.2. TEG mounting location and methods

The available temperature on the stove's usable surfaces largely determines the location of the TEG on the stove. Other than the stovetop, which would normally be used for cooking, it was found that the side opposite the firebox provided the highest temperature surface. Fig. 4 shows a contour plot of the side temperatures measured using an infrared thermometer (Love Controls Div., Model IR-211). The ambient temperature at the time of recording was 28 °C.
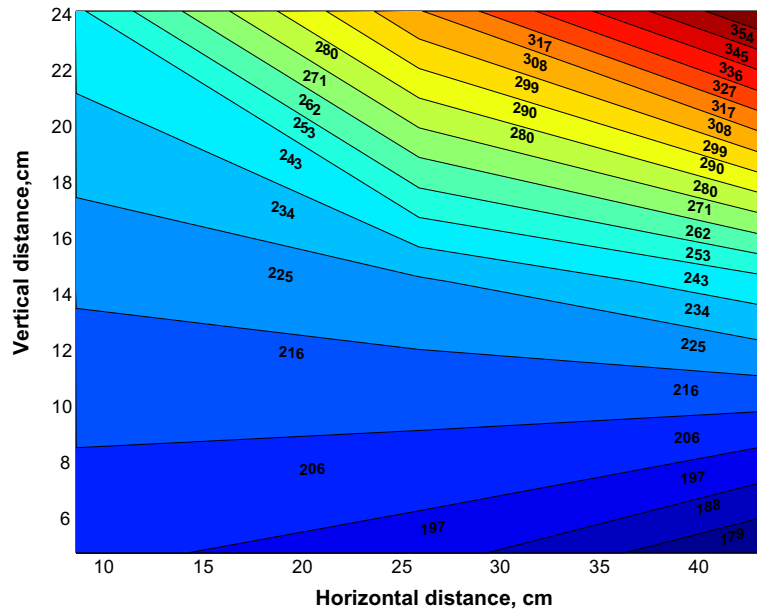
Fig. 4. Measured stove side temperatures (in degrees centigrade) prior to TEG system retrofit. 2.5 kg/h firing rate, 19 °C ambient temperature. Horizontal and vertical distance indicated relative to bottom left corner of stove side.

The isotherms correspond to the flow path of the hot combustion gasses from the firebox (near the top right hand corner) to the fume duct (top left hand top surface). The hottest area is on top of the firebox; the coldest region appears to be below the ash pit (bottom right hand corner). Based on these measurements, it was concluded that the optimal location for the prototype TEG would be near the upper right hand corner of the stove side where the temperatures are at a maximum.

A 1 cm thick smooth aluminum plate was attached to the side of the stove by four screws that were drilled into the stove surface. The aluminum plate was used so that the TEGs will be in contact with a relatively uniform mounting surface. The TEGs were coated with thermal grease at both ends and mounted at the middle of the aluminum plate by pressure applied to them via the heat sink, which, in turn, was held in place by an adjustable clamping mechanism that was fixed into the aluminum plate as shown in Fig. 5.

5.3. Instrumentation

Thermocouples and TEG voltage outputs were connected to a PC based data acquisition system (National Instruments 4036E/4035 high precision temperature and voltage terminal), which recorded one set of readings every 30 s. Grounded stainless steel, sheathed K-type thermocouples were attached at several locations on the stove and chimney. Thermocouples were mounted just below the surfaces of the aluminum plate and heat sink, as shown in Fig. 5. The thermocouples were located along a horizontal line corresponding to the midpoint of the center TEG in the vertical direction. The averages of the three thermocouple temperatures on each side of the TEG were
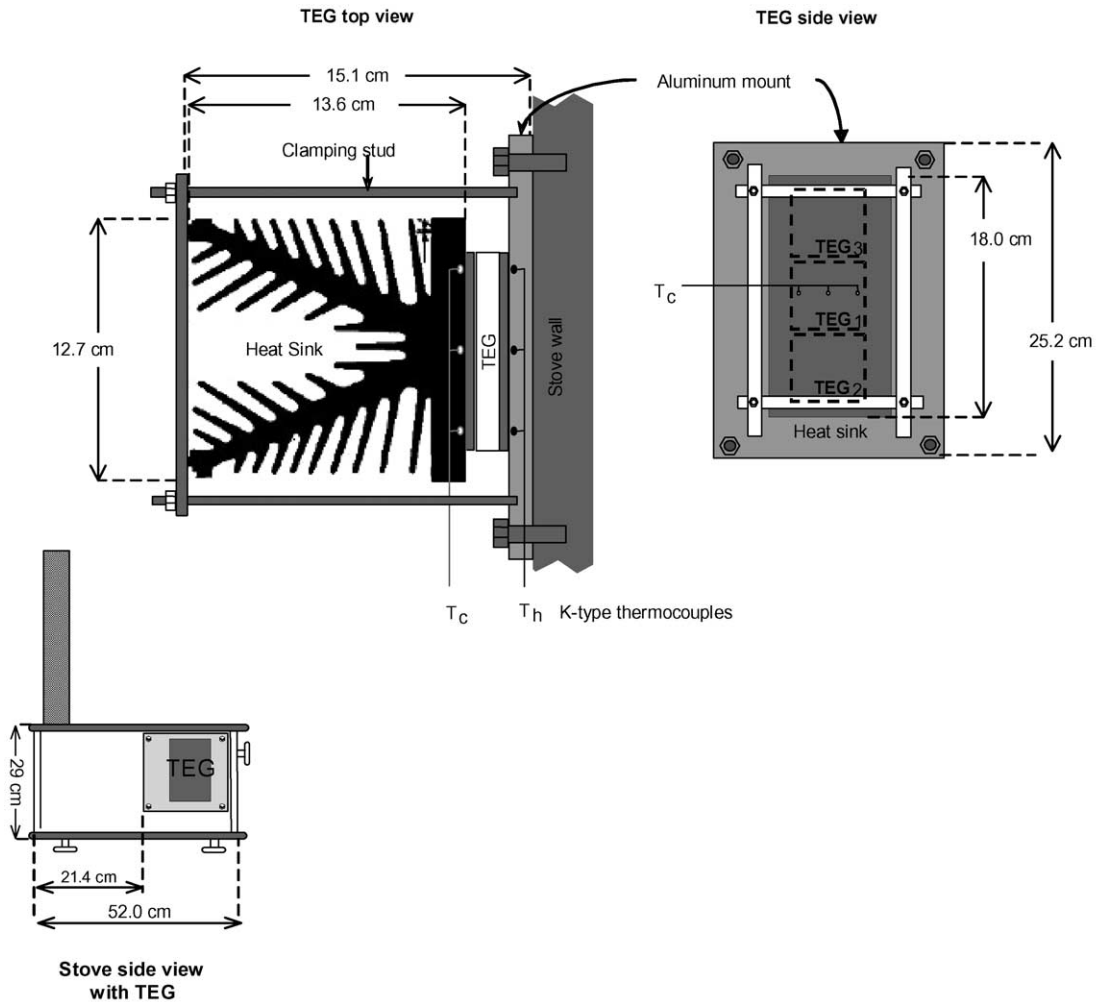
Fig. 5. TEG installation details and location on stove (lower left).

taken as the instantaneous "hot" and "cold" side temperatures, T_H and T_C, respectively. The TEG measurement uncertainties were $\pm 0.5\,^\circ C$ and $\pm 0.01\,V$, based on manufacturer specifications.

The results derived from the experimental measurements are reported with propagation of uncertainty analysis based on a first order Taylor series expansion of the calculated variable, as presented in Figliola and Beasley [10].

5.4. Experimental program

Open circuit voltage outputs, as well as heat source and sink temperatures were measured from start up to 90 min after steady state was achieved. The number of TEG modules mounted under the heat sink was varied from one to three, with the modules electrically connected in series. The steady state wood firing rate was maintained at 2.5 kg/h.

6. Results and discussion

6.1. Transient and steady single TEG module performance

Fig. 6 shows typical measured temperature and voltage profiles at the standard feeding schedule of 2.5 kg/h and an ambient temperature of 19 °C. It can be seen in Fig. 6 that the open circuit voltage closely follows the temperature difference between the mounting plate and heat sink base. After approximately 100 min, the stove operation stabilizes, giving an average hot side temperature of 275 °C and cold side temperature of 123 °C. For this temperature difference of 152 ± 0.7 °C, the TEG produces an open circuit voltage of 4.1 V, indicating that the actual temperature difference imposed on it is only 85.0 ± 0.2 °C.

The substantial difference between the TEG temperature drop of 85 °C and the mounting plate to heat sink drop of 152 °C is likely due to the contact resistance at the four interfaces between the mounting plate and the heat sink. Solving the thermal circuit for the net resistance between the hot mounting plate and TEG cold side at each measurement in the steady state regime yields an approximately constant value of 0.769 ± 0.004 °C/W. Subtracting the TEG resistance of 0.43 °C/W from this total yields the sum of the four interface resistances of 0.339 ± 0.004 °C/W, or 0.083 ± 0.001 °C/W per interface. This result neglects the thermal resistivities of the thin aluminum and ceramic plates, which were calculated to be about two orders of magnitude smaller than the interface resistance. Using typical values for thermal grease resistivity, which was used at the interfaces, an average interface gap thickness of 0.18–0.21 mm is calculated, which is quite possible but which could be reduced by increasing the mounting pressure and/or polishing the surfaces to reduce the average interface gap.

Taking the interfacial resistances into account, 197.7 ± 0.5 W thermal energy is transported from the stove through the heat sink. Given the measured average heat sink base temperature of 123 °C and ambient temperature of 19 °C, this yields a natural convection heat transfer resistance for the heat sink of 0.528 ± 0.004 °C/W, about 20% greater than the manufacturer's specifications. The difference is quite reasonable given that the heat flux is concentrated in the relatively small area where the TEG meets the base, rather than being evenly distributed over the entire heat sink base.
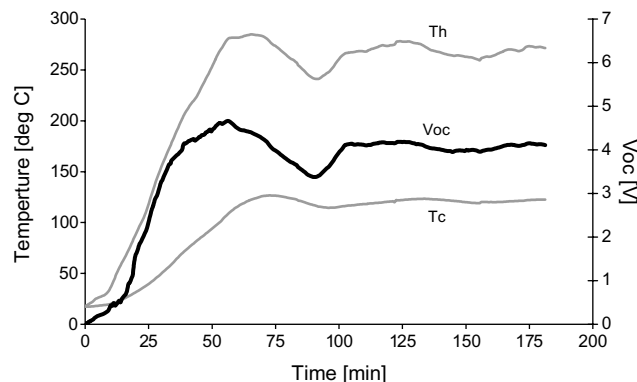

Fig. 6. Open circuit voltage, hot surface temperature T_H and heat sink temperature T_C for single TEG module case versus time. 2.5 kg/h firing rate, 19 °C ambient temperature.

Further, assuming the values for the calculated interface resistances, the TEG hot side temperature is 243 ± 8 °C for the average mounting plate temperature of 275 °C. This indicates that the TEG is nearly optimally located in this configuration since its maximum continuous operating temperature is 250 °C. The only real performance improvement, then, can come from reducing the thermal resistance at the interfaces on the TEG cold side.

6.2. Steady state multi-module performance

The steady natural convection voltages achieved for a varying number of modules is given in Table 3. As shown, while two modules gave a significant increase in voltage over the single module case, the third module produced almost no gain in open circuit voltage despite the predicted increase shown previously in Fig. 2. The deviation from the prediction arises primarily from the assumption in the predictions that $\Delta T_{H\infty}$ remains constant with increasing number of modules. In fact, the hot surface temperature decreases with the increasing number of modules, as shown in Table 3. This is thought to be due to the fact that with an increasing number of modules, the heat transfer rate through the stove surface increases in the vicinity of the TEG, causing a local temperature depression whose magnitude is a function of the stove's internal heat transfer and combustion characteristics. Taking into account the decreasing $\Delta T_{H\infty}$, the predicted and experimental V_{oc} are in good agreement, as shown in Table 3.

Based on the measured open circuit voltage, the single module case provides the highest matched load output of 4.2 ± 0.08 W in steady state operation. While this finding depends on the nature of the combustion and the heat transfer characteristics of the stove, it nonetheless demonstrates that the power output of a TEG with a single heat sink does not necessarily improve with increasing the number of TE modules. The naturally cooled TEG output obtained is comparable to the output reported in a North Sweden study where 5–10 W are produced using two TE modules and a fan cooled heat sink [2].

7. Summary and conclusions

A high performance low cost TEG unit has been designed, built and tested, and the temperature map of a common rural woodstove at an established wood feeding rate has been drawn. This has been done as part of a study to incorporate a thermoelectric generator on the stove in favorable

Table 3
Steady state performance for varied number of modules

Number of modules	$\Delta T_{H\infty}$, $K \pm 0.7$	ΔT_{H-C}, $K \pm 0.7$	ΔT_{TEG}, $K \pm 0.2$	$V_{oc, exp}$	$V_{oc, predicted}$	P_m, $W \pm 0.08$
1	256	152	88	4.1	4.3	4.2
2	250	122	57	5.5	6.3	3.8
3	210	85	41	5.7	6.3	2.7

The temperature drop across the TEG, ΔT_{TEG}, is inferred from the open circuit voltage, V_{oc}. $V_{oc, predicted}$ is calculated using $\Delta T_{H\infty}$, the overall temperature difference from the hot surface to the ambient air. P_m based on calculation from V_{OC}.

regions where electric power supply is subject to prolonged disruption. Using the stove side surface as the heat source, a maximum of 4.2 W per single TEG module has been obtained. For a given heat sink and heat source, increasing the number of TE modules has been shown to *decrease* power output although higher voltages can be realized at some loss in available electric current. Based on the price of the materials purchased in this work, the added cost for more modules may not be warranted with the price per maximum watt for the 1, 2 and 3 module cases rising as 0.24, 0.52 and 1.1 $/W.

In a practical application, the voltages as well as the power need consideration, and this may require more modules, preferably with dedicated rather than shared heat sinks. In general, it has been demonstrated that a form of combined heat and electric power system such as a domestic woodstove-TEG combined system can be achieved at low cost with minimal complexity and a potentially usable output of approximately 4 W per TEG thermoelectric module per heat sink.

Acknowledgement

References

[1] Min G, Rowe DM. Symbiotic application of thermoelectric conversion for fluid preheating/power generation. Energy Convers Manage 2002;43:221–8.
[2] Kilander A, Bass J. A stove-top generator for cold areas. In: Proc 15th International Conference on Thermoelectrics, Pasadena, CA, USA, 1996, p. 390–3.
[3] Nuwayhid RY, Rowe DM, Min G. Low cost stove-top thermoelectric generator for regions with unreliable electricity supply. Renewable Energy 2003;28:205–22.
[4] Iofee AF. Semiconductor thermoelements and thermoelectric cooling. In: Phys Semicond. London: Infosearch Ltd.; 1957.
[5] Rowe DM. Thermoelectric power generation—an update. In: Vincenzini P, editor. 9th Cimtec—World Forum on New Materials, Symposium VII—Innovative Materials in Advanced Energy Technologies, Florence, Italy 1998, p. 649–64.
[6] Slack GA. New materials and performance limits for TE cooling. In: Rowe DM, editor. CRC Handbook on Thermoelectrics. CRC Press; 1994.
[7] Freedman SI. Thermoelectric power generation. In: Sutton GW, editor. Direct Energy Conversion. Mc-Graw-Hill; 1966. p. 141–76.
[8] Melcor Corp., Thermoelectric Engineering Handbook, Trenton, N.J. http://www.melcor.com/handbook.html, last accessed September 15, 2004.
[9] Min G, Rowe DM. Peltier devices as generators. In: CRC Handbook of thermolectrics. London: CRC Press; 1995. Chapter 38.
[10] Figliola R, Beasley D. Theory and design of mechanical measurements. 2nd ed. Wiley & Sons; 1995.